Astron. Astrophys. 96, 296–301 (1981)

ASTRONOMY
AND
ASTROPHYSICS

Dynamic Spectra of Some Terrestrial Ionospheric Effects at Decametric Wavelengths Applications in Other Astrophysical Contexts

N. Meyer-Vernet*, G. Daigne**, and A. Lecacheux**
Observatoire de Paris-Meudon, F-92190 Meudon, France

Received July 15, accepted August 22, 1980

Summary. Ionospheric perturbations in the dynamic spectra of solar and jovian radio emission in the decametric range are presented. A theoretical interpretation is given in terms of focusing and diffraction by large scale ionospheric inhomogeneities, namely quasi-periodic travelling disturbances producing large phase changes.

The interpretation does not involve ad-hoc parameters; it takes into account the source size and gives the effects on the visibility function.

Other astrophysical situations where such an approach would be useful are shortly discussed: similar effects could account for some broad-band interplanetary scintillations observed recently; in addition, it is suggested that propagation effects through the jovian plasma torus could serve to interpret unexplained features of the Jupiter radio emission.

Key words: scintillation – travelling ionospheric disturbances – Sun – Jupiter – radio bursts

I. Introduction

Terrestrial ionospheric propagation effects on radio observations have been studied for a long time. A great deal of work has been done on the scintillations ascribed to random electron density irregularities with a broad spectrum involving spatial scales as low as some tenth of kilometers (see the review by Crane, 1977). Some observations which obviously did not fit with this interpretation have been ascribed to isolated density irregularities (Titheridge, 1971a; Davies, 1980) or wave-like ones (Warwick, 1964). The effects of wave-like travelling ionospheric disturbances (TID) due to gravity waves of medium scale ($\sim$100 km; period $\sim$20 mn) were identified on solar radio bursts position at metric wavelengths (Litva, 1972; Bougeret, 1980). Since these are a regular daily feature and the focusing distance may correspond to an earth-bound observer at decametric wavelengths, these disturbances are expected to perturb the observations of intensity as well as source size, and the corresponding effects have been calculated analytically (Meyer-Vernet, 1980).

In order to relate quantitatively the observations to the effects of ionospheric inhomogeneities, the so-called "dynamic-spectrum" (which displays the intensity in the time-frequency plane) is an important tool. Up to now it has not been very much used for ionospheric scintillation studies (Wild and Roberts, 1956; Warwick, 1964).

In this paper we present dynamic spectra obtained in the decametric range. They clearly show effects of ionospheric perturbations on the incoming radiation. The observed sources are the Sun and the planet Jupiter with different kinds of radio emission.

A theoretical interpretation involving a ionospheric gravity wave is then given. The model, as simple as possible for the gravity wave, takes into account the source size and shows that different effects are to be expected (and observed) on solar and jovian emissions. Then it predicts the corresponding effects on the measurements of source's visibility.

II. Observations

The observations were performed with the decametric arrays at Nançay (Boischot et al., 1980), formed of two independent sets of seventy-two broadband conical helical antennas sensitive to opposite senses of circular polarisation. The gain of each array is nearly 25 dB, independent of the frequency in the range 10 to 110 MHz.

Each array is connected to sweep-frequency spectrographs with adjustable characteristics. For solar observations the 25–75 MHz frequency range is scanned with a frequency resolution of 100 kHz and for jovian observations the frequency range is 10–40 MHz with a 30 kHz resolution.

The output intensity is recorded on film with a double track corresponding to each array. The observations of the Sun and Jupiter are performed daily for three hours apart from the transit time.

The dynamic spectrum of the jovian decametric emission usually exhibits various kinds of curved fringe systems and other spectral features, a number of which are obviously not of jovian origin because of the absence of correlation with the jovian rotation or Io's effect.

The quiet Sun cannot be studied with the system in use; as the active Sun is a sporadic source with a wide range of spectral features, only very strong and peculiar effects of ionospheric disturbances could have been identified from our observations at a single location.

Figure 1a, b shows two examples of perturbed dynamic spectrum ascribed to ionospheric effects on solar emission. In each case a solar noise storm is observed, strongly polarized in the left-handed sense.

Similar kinds of spectral features occurred during the same observing period (december 1979 to march 1980). Generally, one

Send offprint requests to: N. Meyer-Vernet
* LA C.N.R.S. No. 264
** Groupe de radioastronomie décametrique

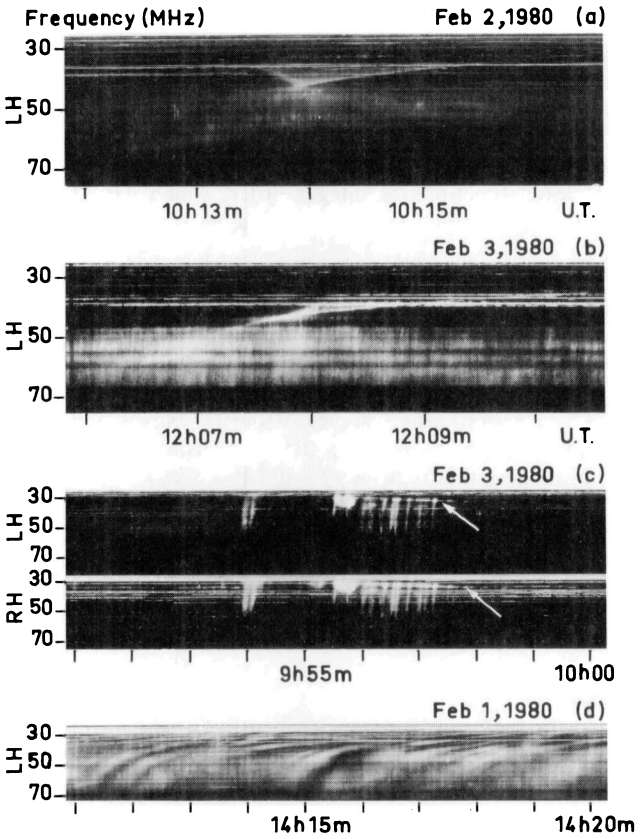

Fig. 1a–d. Observed dynamic spectra of solar radio emissions, showing ionospheric perturbations. **a** caustic figure on a solar noise storm strongly *LH* circularly polarized. **b** similar event with a stronger asymmetry. The output intensity of the spectrograph is in linear scale, instead of logarithmic scale as usual. **c** group of Type III bursts with a slow drifting band of brightness increase. There is a slight frequency shift between the two bands observed in opposite sense of polarization. **d** modulation pattern of a solar noise storm. This kind of modulation is rather unusual in solar observations. It is still ascribed to ionospheric perturbations because of the typical periodicity ($\simeq$20 mn) of the perturbations for this day

or two slowly drifting bright bands of emission in the low frequency range are accompanied by a smoother brightness increase in the middle frequency range. The characteristic time interval between such features is about 25 or 30 min. It strongly suggests a ionospheric effect as already mentioned for other day-time observations (e.g., solar bursts position measurements, see Bougeret, 1980).

For the observation of Fig. 1a, b, the source size is expected to be about 1–10′ depending on the frequency, and the zenith angle is $\sim 66°$. The patterns show a focal region around the frequency 43 MHz, and a marqued asymmetry.

It has to be noted that most often spectral features with a single branch were observed on solar radio emission, as shown in Fig. 1c. Here a group of type III bursts display an intensity increase along a slowly drifting band. The frequency drift of this band is of the order of the frequency drifts observed in other cases of solar activity (type II bursts or chains of type I bursts), thus, it could possibly be interpreted as a purely solar phenomenon. However, this kind of feature shows the same repetition pattern as already mentioned (20–30 mn periodicity) and, furthermore, the two bands of opposite circular polarisation are slightly shifted in frequency, following the rule $f_{RH}-f_{LH}\sim 0.8$ MHz. This value is typical of the other similar observed events. It is not clear whether the feature reported in Fig. 1c is a part of a caustic pattern which could not have been fully observed because of a lack of solar emission at the time of best focusing, or whether it is the result of some asymmetry in the focusing process. This question will be discussed later on. First the theoretical model deals with the observations reported in Fig. 1a, b, which are the most valuable.

III. Theoretical Interpretation

The characteristics of the observed phenomena suggest an interpretation involving a wave-like ionospheric disturbance of medium scale. In this section we recall some heuristic results, then we give a simplified model and the computed results.

III.1. Heuristic Results

Consider an inhomogeneity of spatial scale d, which is assumed to impose a phase change $\Phi \gg 1$ on the incoming radio waves. For a wave-number $k_0 = 2\pi f/c$, the corresponding angular deviation is $\delta\theta \sim \Phi/k_0 d$ and the "focusing" distance is nearly $z_F \sim d/\delta\theta$.

Consider a source at infinite distance, observed at distance z behind the disturbance; if $z \ll z_F$, only angular refraction is observed, but for $z \gtrsim z_F$, focusing and diffraction must be considered and the intensity and visibility are modified accordingly. Broadly speaking, geometrical optics predicts that, behind the "focus", the intensity is concentrated (for a converging lens-like irregularity) within the transverse distance $|x| \sim \delta\theta(z - z_F)$ or, if the irregularity moves with the transverse velocity v: $|\Delta t| \sim (d - z\delta\theta)/v$. Since $\Phi \propto f^{-1}$ and $\delta\theta \propto f^{-2}$, this yields the slope of the pattern in the time-frequency plane:

$$|df/dt| \sim vf/2\, z\delta\theta. \tag{1}$$

If the source is sufficiently small, i.e. its angular size $\Delta\theta_s$ satisfies:

$$z\Delta\theta_s < 1/k_0\delta\theta \tag{2}$$

there are diffraction fringes of spatial scale Δx satisfying $k_0 \Delta x \delta\theta \sim 1$. Thus $\Delta x \sim d/\Phi$ and the frequency scale Δf is such that $\partial/\partial f(z\delta\theta) \sim \Delta x/\Delta f$ (or $\Delta f \sim (z\delta\theta^2/c)^{-1}$). We obtain:

$$\Delta f/f \sim d/2\,\Phi z\delta\theta. \tag{3}$$

This heuristic value is analogous to the known expression for the decorrelation bandwith for random scilnitillations (Salpeter, 1967) as well as the value computed for a sinusoidal screen (Meyer-Vernet, 1980). If the source does not satisfy the inequality (2), the fringes are smeared out.

Some of these results can also be obtained (Ratcliffe, 1956) by reasoning on the irregularity's spectrum, which contains spatial scales extending from d/Φ to d(if $\Phi > 1$).

III.2. The Model and Basis of the Calculation

The model and calculations are given in Meyer-Vernet (1980), as well as the limitiations. The main features are the following: the

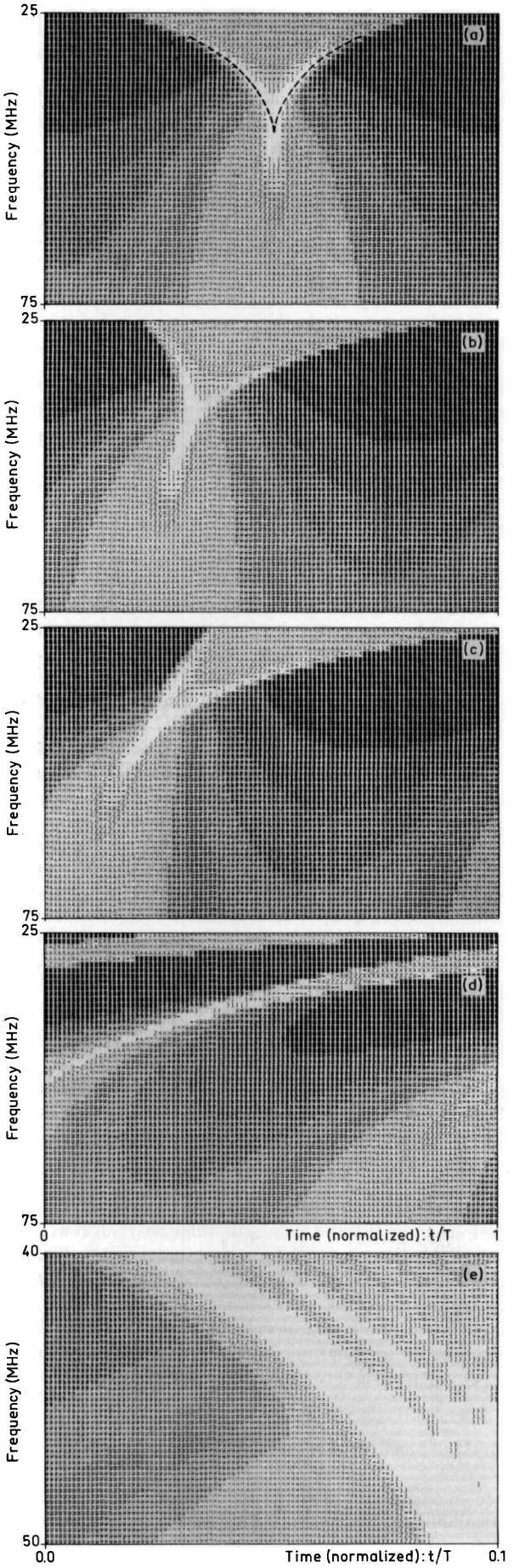

travelling ionospheric disturbance is approximated by a one-dimensional thin phase-screen $\Delta\Phi(x, t)=\Phi_0 \cos((x-vt)/d)$; the parameters satisfy $\Phi_0 \gg 1$, $\delta\theta=\Phi_0/k_0 d \ll 1$, $k_0 d \gg 1$, and $\Phi_0 Z=\Phi_0 z/k_0 d^2 \sim 1$; the calculation is done in the usual Fresnel approximation and the visibility for a given source is obtained as a single sum of Bessel functions of integer order, which permits easy numerical computations, even for high values of Φ_0.

III.3. The Parameters of the TID

We take the following typical values (Yeh, 1974): wavelength $2\pi d \sim 100$ km (a typical equivalent velocity of 50–100 m/s gives the observed period); the distance of the F_0F_2 layer ~ 300 km, with the inclination of 24° gives the slant distance $z \sim 750$ km. The focusing near the frequency $f \sim 40$ MHz needs taking $\Phi_{0(\mathrm{rad})} \sim 1.5\ 10^4/f_{\mathrm{MHz}}$. Given a typical mid-latitude daytime total electron content in february (and near the solar activity maximum) of $4\ 10^{17}$ e-m^{-2}, this yields a relative density disturbance of about 4%; which is important but not unusual for the period considered (Titheridge, 1971b).

III.4. Calculated Results

Figure 2a shows the theoretical dynamic spectrum obtained with the above parameters and a source size of 10′ at $1/e$ power (as inferred from Sect. II). The pattern is of course symmetric but it is expected that, at the local time considered, the wave is actually superimposed on a density gradient; furthermore, the TID are known to be tilted. The simplest hypothesis is to take a constant gradient $d\Phi/dx=\alpha(\propto f^{-1})$. Then, it can be easily shown that the observed visibility function at lateral location x and time t is deduced from its value for $\alpha=0$ as:

$$V_{\substack{\mathrm{obs}\\ \alpha\neq 0}}(a, x, t)=V_{\substack{\mathrm{obs}\\ \alpha=0}}(a, x, t+\alpha z/k_0 v). \tag{4}$$

Taking increasing values of α yields the dissymetric patterns shown in Fig. 2b and c. These compare well with the corresponding measured patterns displayed in Fig. 1a and b.

Finally, for higher values of α, only one caustic branch is visible in one period, as shown in Fig. 2d, to be compared with the experimental Fig. 1c.

Fig. 2a–e. Theoretical dynamic spectra for a source seen through a (simplified) travelling ionospheric disturbance. The observing frequency is indicated (in MHz) on the left side, and the time (in abscissae) is normalized to the disturbance's period $T=2\pi d/v$. The intensity (normalized to the undisturbed one) is displayed using a grey shading level scale ranging from 0.5 (dark) to 6 (white). **a** Source size $\Delta\theta_s=10'$; phase-change: $\Phi_0=1.5\ 10^4/f_{\mathrm{MHz}}$; wavelength $2\pi d=100$ km, distance $z=300$ km/sin 24°. One period of the disturbance is displayed. **b** Same parameters as in **a** with a superimposed phase-gradient $\alpha=-0.1\times 2\pi\Phi_0/d$. **c** Same parameters as **a**, with $\alpha=-0.2\times 2\pi\Phi_0/d$. **d** Same parameters as **a**, with $\alpha=-0.6\times 2\pi\Phi_0/d$. **e** The source is sufficiently small so that diffraction fringes appear. One tenth of period of the disturbance is displayed. Source size $\Delta\theta_s=1'$ ($\Phi_0=5\ 10^3/f_{\mathrm{MHz}}$; $2\pi d=50$ km, z as in **a**–**d**

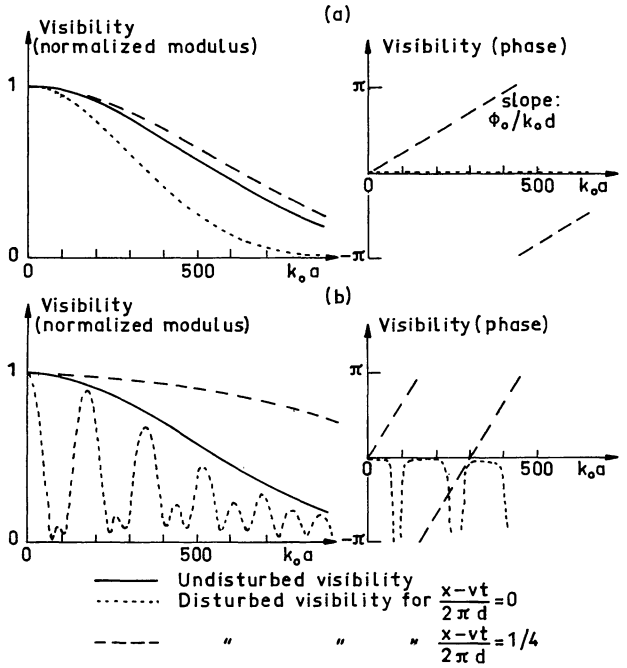

Fig. 3a and b. Calculated visibility curves with the parameters as in Fig. 2a at frequencies $f=75$ MHz **a** and $f=35$ MHz **b**

It is worth noting that for the above parameters (particularly, the large source size), geometrical optics yields good results, as shown in Appendix 1.

IV. Discussion

IV.1. Comparison between Theory and Experiment

There is a good overall agreement, in spite of the simplicity of the model. We stress that the theory has few free parameters and that we have chosen typical values, without doing peculiar efforts of fitting, neither introducing ad-hoc hypotheses.

Of course, the model could be refined, since it is a very crude approximation of an actual T.I.D.; one should introduce higher-dimensional features and actual assymetries of the disturbance, and the source size and position is expected to be frequency dependent; in addition, oblique incidence should be taken into account (see Appendix 2). In particular, a two dimensional model for the T.I.D. might be useful to interpret the case of Fig. 1c) which seems to be the most usual. In such a case the observing plane defined by the line of sight and the apparent speed of the T.I.D. would intersect a caustic surface and not necessarily contains the focal point; so, only one branch of the caustic would be observed in the dynamic spectrum.

Anyway, we believe that the present model contains the main physics of the real situation.

We note that it must not be applied for distances $z \gg z_F$ since, then, too many periods of the sinusoidal disturbance would contribute to the observed pattern, and the finiteness of the disturbance should be taken into account.

Finally it is worth noting that the calculation neglects the effects of the magnetic field; a short evaluation shows that the observed shift in frequency between the two circular polarisation components is consistent with the present interpretation: the phase difference between the two propagating modes is $\Delta\Phi_0 \sim 2\Phi_0 f_H \cos\theta/f$ (where f_H is the gyrofrequency and θ the angle of propagation with the magnetic field). Thus, with typical parameters ($\theta \sim 45°$, $f_H \sim 1$ MHz), $\Delta(\Phi_0 Z)/(\Phi_0 Z) \sim \sqrt{2}/f_{\text{MHz}}$; this yields the approximate frequency polarisation shift: $\Delta f \sim 0.7$ MHz, which is nearly the observed result.

IV.2. Lowering the Source Size

The sources involved above satisfy: $z\Delta\theta_s \gg 2\pi d/\Phi_0$, so that the diffraction fringes are smeared out and only a caustic-like pattern is seen. If the source is smaller, fringes appear, as shown in Fig. 2e, which corresponds to a case where $z\Delta\theta_s \sim 2\pi d/\Phi_0$ (and $\Delta\theta_s < \delta\theta$). As the source becomes smaller, more fringes appear, yielding finally a pattern as shown in Meyer-Vernet (1980) in the limit $\Delta\theta_s \to 0$.

In some rare cases, when the source is the Sun (Fig. 1d) and in most cases, when the source is Jupiter (Fig. 5a), the observations exhibit such fringes. Indeed, with the present parameters, Jupiter's source acts as a point source [inequality (3)], and the interpretation gives the correct fringes spacing. However, there is not here such a good overall agreement between theory and experiment as between Fig. 1a, b, c and Fig. 2b, c, d; Fig. 2e shows only a part of the computed dynamic spectrum, the other part of which showing a pattern in the reverse sense.

A good agreement should involve refinements of the model, as outlined above. Furthermore, by night-time (when the lowest frequency observations of Jupiter are made) the effect of such a gravity wave considered here is known to be less important and other type of disturbances (not wavelike ones and/or with a smaller spatial scale) should be taken into account.

IV.3. Consequences on Visibility's Measurements

The present results have interesting consequences for the interferometric measurements. Figure 3 shows the theoretical visibility function for a 10′ source seen through the disturbance discussed in the previous section. At 75 MHz, only the source position is strongly perturbed; at 40 MHz, the observed source shape is also perturbed and the measurement depends strongly on the interferometer used. The measured source size may be larger or smaller than the actual one or multiple, though the integration time and/or bandwidth may often be too large for the latter cases to occur in practice.

V. Conclusion

We have presented some solar and jovian dynamic spectra obtained at Nançay in the decametric range. They show scintillation patterns interpreted in terms of propagation effects through typical travelling ionospheric disturbances involving large phase changes.

The interpretation which were previously done for this kind of scintillations were only heuristic (Warwick, 1964), or did not involve an entire broadband dynamic spectrum (see, for instance, Heron, 1976). The present one gives an attractive explanation of many spectral structures observed usually in the 20–75 MHz frequency range. Our approach is quantitative. It involves broadband dynamic spectrum comparison between observations and theory with only few free parameters, and takes the source size

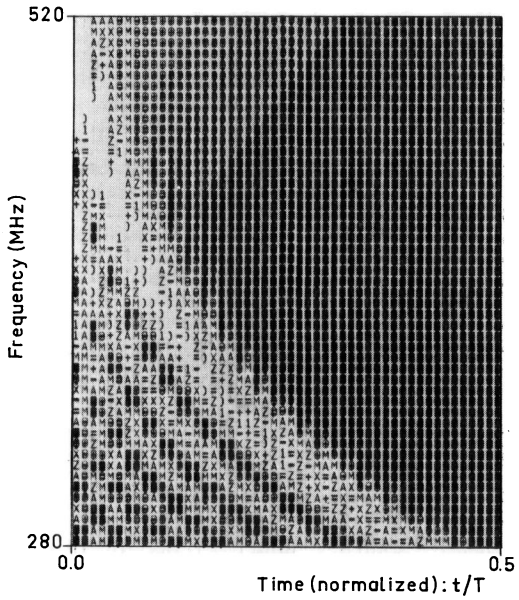

Fig. 4. Theoretical dynamic spectrum for a radio-source (size $\lesssim 0''.05$) seen through a sinusoidal disturbance in the solar wind. Phase-change $\Phi_0 = 10^4/f_{(\mathrm{MHz})}$; wavelength $2\pi d = 3000$ km; distance $z = 1$ A.U. One half of period is displayed, corresponding to a time duration $T/2 = \pi d/v \sim 3.7$ s (with a typical solar wind speed $v \sim 400$ km s^{-1}). The pattern exhibits some similarity with the observations by Cole and Slee (1980)

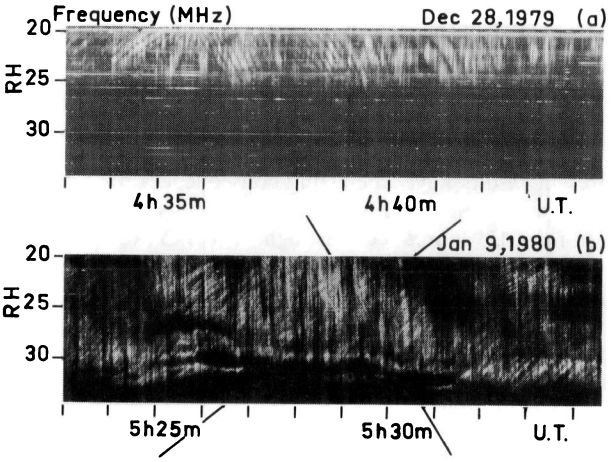

Fig. 5a and b. Dynamic spectra of jovian radio emission showing different fringe patterns ascribed to propagation effects in low plasma density. **a** Typical pattern observed in ionospheric scintillations of small size radio sources. **b** Complex pattern of modulation lanes with positive and negative frequency drifts

into account: small sources yield diffraction fringes, while larger sources yield only a caustics-like pattern.

Similar effects should appear in other astrophysical situations: in particular, in some cases of interplanetary scintillation and in the propagation of the decametric radiation near Jupiter.

Broadband dynamic spectra of interplanetary scintillations were recently published (Cole and Slee, 1980). They show patterns rather similar to the ones reported in this paper for a small source. The solar wind irregularities are thought to have a power-law spectrum; Hewish (1980) argues that "small-scale irregularities combined with phase-gradients due to large-scale irregularities" should produce the observed patterns. Figure 4 shows the theoretical dynamic spectrum given by the model described in Sect. III-2 with parameters of the order of those considered by Hewish for large-scale inhomogeneities. One half of period is displayed. The pattern exhibits much similarity with the reported scintillations.

This suggests that large-scale inhomogeneities as considered in the present paper, or lens-like ones could produce the observed patterns. Such focusing effects have been considered to explain the so-called spikes observed in fixed-frequency records of interplanetary scintillations (Armstrong et al., 1972; Buckley, 1975). The large irregularities can be produced by a random spectrum of scale sizes. However the present deterministic approach is useful for this kind of scintillation: if the number of realizations is too small, the statistical averages usually computed in IPS studies are irrelevant.

The jovian decametric radio emission is known to have a complex dynamic spectrum with mixed fringes systems in the frequency-time plane. Some are due to the propagation through the terrestrial ionosphere (Fig. 5a), but the so-called modulation lanes (Riihimaa, 1970) are believed to have a jovian origin (Fig. 5b), unexplained at the present time. The modulation lanes appear as groups of drifting fringes with typical duration of an hundred of seconds and quasi-periodicity of 3 s. The slope of the lanes, nearly 100 kHz s^{-1}, reverses around the system III 200° longitude, which is the major indication for a jovian origin.

Some authors (Green and Gurnett, 1980; Lecacheux, 1981) pointed out that the refraction of the emitted radiation through the Io plasma torus is able to modify significantly the directivity of the jovian low frequency emission. In addition we suggest that the Io-torus could introduce diffraction effects up to the decametric range. The corresponding plasma introduces a (negative, i.e. diverging lens-like) phase-change of order $\Phi_0 \sim 10^6/f_{\mathrm{MHz}}$; with the typical latitudinal scale $d \sim 0.1\ R_J$, where R_J is planet Jupiter radius and distance $z \sim 4\ 10^8$ m (in this problem, z is the distance source – screen, since the observer's distance is much higher), the parameter $\Phi_0 Z$ is of order 1 in the decametric range. This yields, for a source sufficiently small (spatial size $\Delta X_s \lesssim 2\pi d/\Phi_0 \sim 2\ 10^3$ m) a diffraction pattern of time-scale $T/\Phi_0 \sim 1$ s (where $T \sim 10$ h is the period of variation of the geometrical conditions of propagation along the Jovian rotation) and typical slope given by (1), thus $|1/f\ df/dt| \sim 2\ 10^{-4}$ s^{-1} (where $v \sim 1\ R_J/T$). These values are in agreement with the observations.

This order of magnitude estimate indicates that it should be interesting to extend the present approach, with a correct description of the Io torus.

Such propagation effects, which were previously not considered, could play a major role in the observed and unexplained properties of the jovian radio emissions. They are presently under study.

References

Armstrong, J.W., Coles, W.A., Rickett, B.J.: 1972, *J. Geophys. Res.* **77**, 2739
Boischot, A.: 1980, submitted to *Icarus*
Bougeret, J.L.: 1981, *Astron. Astrophys.* (in press)
Buckley, R.: 1975, *J. Atmos. Terr. Phys.* **35**, 263
Cole, T.W., Slee, O.B.: 1980, *Nature* **285**, 93

Crane, R.K.: 1977, *Proc. Inst. Elec. Electron. Engrs.* **65**, 180
Davies, K.: 1980, *Space Sci. Rev.* **25**, 357
Green, J.L., Gurnett, D.A.: 1980, *Geophys. Res. Letters* **7**, 65
Heron, M.L.: 1976, *J. Atmos. Terr. Phys.* **38**, 1027
Hewish, A.: 1980, *Nature* **285**, 95
Lecacheux, A.: 1981, *J. Geophys. Res.* (in press)
Liva, J.: 1972, in AGARD conf. proceed. no. 115, 27-1
Meyer-Vernet, N.: 1980, *Astron. Astrophys.* **84**, 142
Ratcliffe, J.A.: 1956, *Rep. Prog. Phys.* **19**, 188
Riihimaa: 1970, *Astron. Astrophys.* **4**, 180
Salpeter, E.E.: 1967, *Astrophys. J.* **147**, 433
Titheridge, J.E.: 1971a, *J. Atmos. Terr. Phys.* **33**, 47
Titheridge, J.E.: 1971b, *Planetary Space Sci.* **19**, 1593
Yeh, K.C., Liu, C.H.: 1974, *Rev. Geophys. Space Phys.* **12**, 193
Warwick, J.W.: 1964, *Radio Sci. J. Res. NBS* **68D**, 179
Wild, J.P., Roberts, J.A.: 1956, *J. Atmos. Terr. Phys.* **8**, 55

Appendix 1: Geometric Optics Calculation

In the two-dimensional coordinates x, z, the ray equation is given by:

$$\frac{1}{k_0}\frac{d\Phi}{dX}=\frac{x-X}{z}$$

where X is the entry point on the screen and $\Phi(X)=\Phi_0\cos\left(\frac{X-vt}{d}\right)$.

Thus, the caustics equation is given by:

$$\begin{cases} F(x, z, X)=0 \\ \partial F/\partial X \quad =0 \end{cases}$$

where

$$F(x, z, X)=\Phi_0 Z \sin\left(\frac{X-vt}{d}\right)+\frac{x-X}{d}$$

and

$$Z=z/k_0 d^2.$$

Thus, the intensity in the dynamic spectrum is maximum on the curve (in parametric coordinates):

$$\begin{cases} 2\pi t/T-x/d=\varphi-\text{tg}\,\varphi \\ \Phi_0 Z \qquad\quad =1/\cos\varphi \end{cases}$$

(where $\varphi=(X-vt)/d$).

This curve is shown in dotted-line in Fig. 2a.

Appendix 2: Oblique Incidence

In the Fresnel approximation, the field at (x, z) can be written as:

$$E(x, z)\propto \int dX E(X, 0^+)\exp(ik_0 u)$$

where

$$E(X, 0^+)=E(X, 0^-)\exp(i\Phi(X))$$

is the field emerging from the screen and:

$$u=[(x-X)^2+z^2]^{1/2}\simeq z/\cos\theta+(X-x-z\,\text{tg}\,\theta)\sin\theta + (X-x-z\,\text{tg}\,\theta)^2\cos^3\theta/2$$

(θ is the incidence angle; small deviations from θ are assumed, and unnecessary factors have been omitted). Thus, it is easily shown that the visibility at x, z is given by the expression found in the case of normal incidence, at coordinates:

$$x'=x+z\,\text{tg}\,\theta, \qquad z'=z/\cos^3\theta.$$

This increases sharply the effective distance z and thus the parameter Z. However, in this case, higher-dimensional features are likely to be important.